



# OPEN Bone conduction stimulation efficiency at coupling locations closer to the cochlea

Irina Wils<sup>1</sup>✉, Alexander Geerardyn<sup>1,2</sup>, Guy Fierens<sup>3</sup>, Tristan Putzeys<sup>1,4,6</sup>, Kathleen Denis<sup>5,6</sup> & Nicolas Verhaert<sup>1,2,6</sup>

Bone conduction implants enable patients to hear via vibrations transmitted to the skull. The main constraint of current bone conduction implants is their maximum output force level. Stimulating closer to the cochlea is hypothesized to increase efficiency and improve force transfer, addressing this limitation. This study evaluated stimulation at four positions in human cadaveric specimens: the cochlear promontory, the posterior wall of the outer ear canal, the lateral semi-circular canal, and the standard Bone-Anchored Hearing Aid (Baha) location. To assess potential hearing sensation, three objective measures were simultaneously recorded. For intracochlear pressure and promontory velocity, stimulating at the lateral semi-circular canal and promontory results in the highest response, with a gain of up to 20 dB. Ear canal pressure shows less conclusive results, with significant differences at only a few frequencies. These findings suggest that stimulation closer to the cochlea offers higher efficiency, which could benefit patients needing higher output force levels than currently available or those eligible for electro-vibrational stimulation, e.g. a cochlear implant combined with a bone conduction device.

Bone conduction implants (BCIs) present a promising solution for individuals experiencing conductive, mixed, or sensorineural hearing impairments<sup>1,2</sup>. Unlike conventional air conduction (AC), which relies on sound waves traveling through the ear canal to vibrate the eardrum and ossicles, bone conduction (BC) involves perceiving sound through vibrations transmitted directly to the skull<sup>1</sup>. From the skull, the vibrations reach the cochlea, or inner ear, through five known pathways as described by Stenfelt<sup>3</sup>: (1) through ear canal compression, (2) due to the motion of middle ear ossicles, (3) through cochlear space compression, (4) from the inertia of cochlear fluid, and (5) through secondary fluid paths connecting the inner ear to the cranial cavity. However, details of sound perception through bone conduction largely remain theoretical, with uncertainties surrounding the significance and relative contributions of these pathways<sup>4,5</sup>.

Utilizing these pathways, BCIs are effective for individuals with a BC pure tone average of up to 45 dB for most transcutaneous devices<sup>6–9</sup>, where the internal and external parts of the devices are connected using a magnet on either side of the skin<sup>10</sup>. In contrast, or some percutaneous devices, where both parts of the device are connected through a skin penetrating abutment, the inclusion criteria even go up to 55–60 dB<sup>10</sup> hearing loss, according to the manufacturer. However, the primary limitation of these devices is their maximum output force level. Increasing this level can enhance speech recognition, better processing of spatial information, and subjective sound quality<sup>11–13</sup>. Another approach to achieve these benefits is to enhance the stimulation efficacy of bone conduction implants, and thus the perceived loudness related to the output force level. This improvement could expand the fitting range and enhance wearing comfort.

Improving current BCIs involves exploring new implantation strategies for enhanced stimulation efficacy, and thus prolonged battery life, or increased output. One potential approach is to position implants closer to the cochlea rather than on the skull surface. Research by Eeg-Olofsson et al.<sup>14</sup> and Niemczyk et al.<sup>15</sup> has shown that stimulating nearer to the cochlea, specifically on the otic capsule, results in increased movement and velocity of the promontory – the surface of the cochlea between the stapes and round window. This proximity also reduces transcranial transmission and improves signal separation, which aids in sound localization<sup>16</sup>. Positioning the device near the cochlea is challenging because it requires the fixation of a vibrating mass inside the limited

<sup>1</sup>Department of Neurosciences, Research Group Experimental Oto-rhino-laryngology, KU Leuven, Leuven B3000, Belgium. <sup>2</sup>Department of Otorhinolaryngology, Head and Neck Surgery, University Hospitals Leuven, Leuven B3000, Belgium. <sup>3</sup>Cochlear Technology Center, Mechelen B2800, Belgium. <sup>4</sup>Department of Physics and Astronomy, Laboratory for Soft Matter and Biophysics, KU Leuven, Leuven B3000, Belgium. <sup>5</sup>Department of Mechanical Engineering, Biomechanics Section, KU Leuven, Leuven B3000, Belgium. <sup>6</sup>These authors jointly supervised this work. ✉email: irina.wils@kuleuven.be

mastoid cavity, and is in proximity to critical structures such as the facial nerve, several blood vessels, and the cochlea itself<sup>17</sup>. However, it is particularly intriguing for electro-vibrational stimulation<sup>18</sup>, where it is combined with a cochlear implant and where positioning a BCI closer to the cochlea does not make the surgery more invasive.

Due to the invasive nature of BCIs, whether percutaneous or transcutaneous, they require preclinical evaluation on cadaveric specimens before patient trials<sup>19</sup>. Unlike live patient feedback, cadaveric tests rely solely on objective measures. Presently, three metrics are commonly employed. Intracochlear pressure<sup>20–25</sup> involves measuring the pressure in two cochlear ducts of the inner ear. Since the differential pressure correlates well with the cochlear drive, this measure can be used to estimate hearing sensation<sup>21,26–29</sup>. Promontory velocity<sup>16,25,30–37</sup> is measured with laser Doppler vibrometry (LDV), the current standard for evaluating middle ear implants<sup>38</sup> and it captures the movement of the cochlea, an important factor in bone conduction hearing<sup>3,16</sup>. Lastly, ear canal pressure<sup>25,39,40</sup> may serve as a suitable measure to evaluate bone conduction hearing since ear canal compression is one of the BC pathways, and other pathways might contribute to this pressure via reverse stimulation<sup>16</sup>. These measurements range from an invasive method, which is proximal to the hearing sensation site, to a non-invasive, but more peripheral method<sup>25</sup>.

This study applied bone conduction stimulation close to the cochlea in different surgically feasible and easily accessible areas. It is hypothesized that stimulating closer to the cochlea will produce a louder hearing sensation with the same force level or, alternatively, that less force will be required to achieve the same hearing sensation. Three stimulation locations were selected: the promontory, the semi-circular canal, and the posterior wall of the ear canal as illustrated in Fig. 1. The promontory was chosen since the velocity of this structure relates to the intracochlear pressure, and consequently, auditory sensation. The semi-circular canal was selected since its surface is also part of the otic capsule, which moves differently from the rest of the temporal bone and skull<sup>36</sup>. In addition, it is more distant from delicate structures such as the stapes and round window. Finally, the posterior wall was included since it has an important role in the BC pathways, although it is more distant from the otic capsule. In addition, BC stimulation was also performed at the standard Baha position<sup>41</sup>, to provide a baseline.

Stimulation was provided with an experimental setup, comprising a shaker, an impedance head, and a custom-made rod. The impedance head facilitates the measurement of the output force level generated by the shaker, thereby enabling the normalization of measurement results and ensuring a repeatable and consistent comparison. To acquire an in-depth comparison between BC stimulation at different locations, the three identified objective measures – intracochlear pressure, promontory velocity, and ear canal pressure – are measured simultaneously.

## Results

### Efficiency of stimulation positions

When stimulating close to the cochlea compared to the standard Baha position, the findings demonstrate a gain of up to 20 dB in intracochlear pressure, promontory velocity, and ear canal pressure. These effects are illustrated in Figs. 2 and 3, which show the median, interquartile, and individual gains. It also reveals significant differences through a Friedman test and subsequent post-hoc Tukey analysis. The corresponding p-values from the statistical tests are available in Supplementary Tables S1–S5. Additionally, individual specimen data are comprehensively presented in Supplementary Figs. S9–S13.

#### *Scala vestibuli pressure*

Regarding scala vestibuli pressure, stimulation at the lateral semi-circular canal produces the highest response, particularly for frequencies between 250 and 1000 Hz, where the increase ranges from 15 to 20 dB. This increase

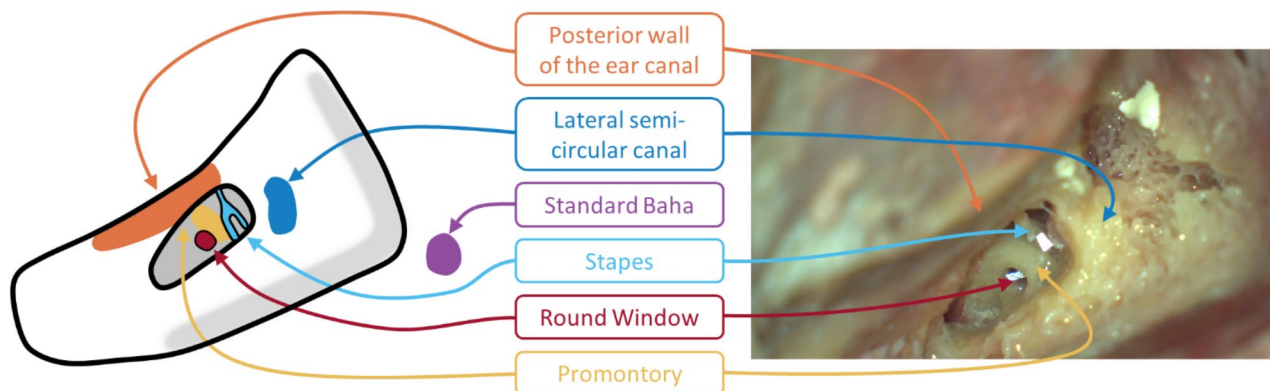


**Fig. 1.** Close-up view of the posterior tympanotomy of a left ear displaying four stimulation positions: the standard Baha position, the lateral semi-circular canal, the promontory, and the posterior wall of the ear canal, along with the anatomical landmarks of the stapes and the round window. Left: schematic representation, Right: microscopic image of the mastoidectomy and posterior tympanotomy, the standard Baha position is not visible on this scale. Retroreflective tape is visible on the stapes and round window in the microscopic image. This tape was used during control measurements but was removed for subsequent measurements (see “Methods”).

## Efficiency of stimulation positions

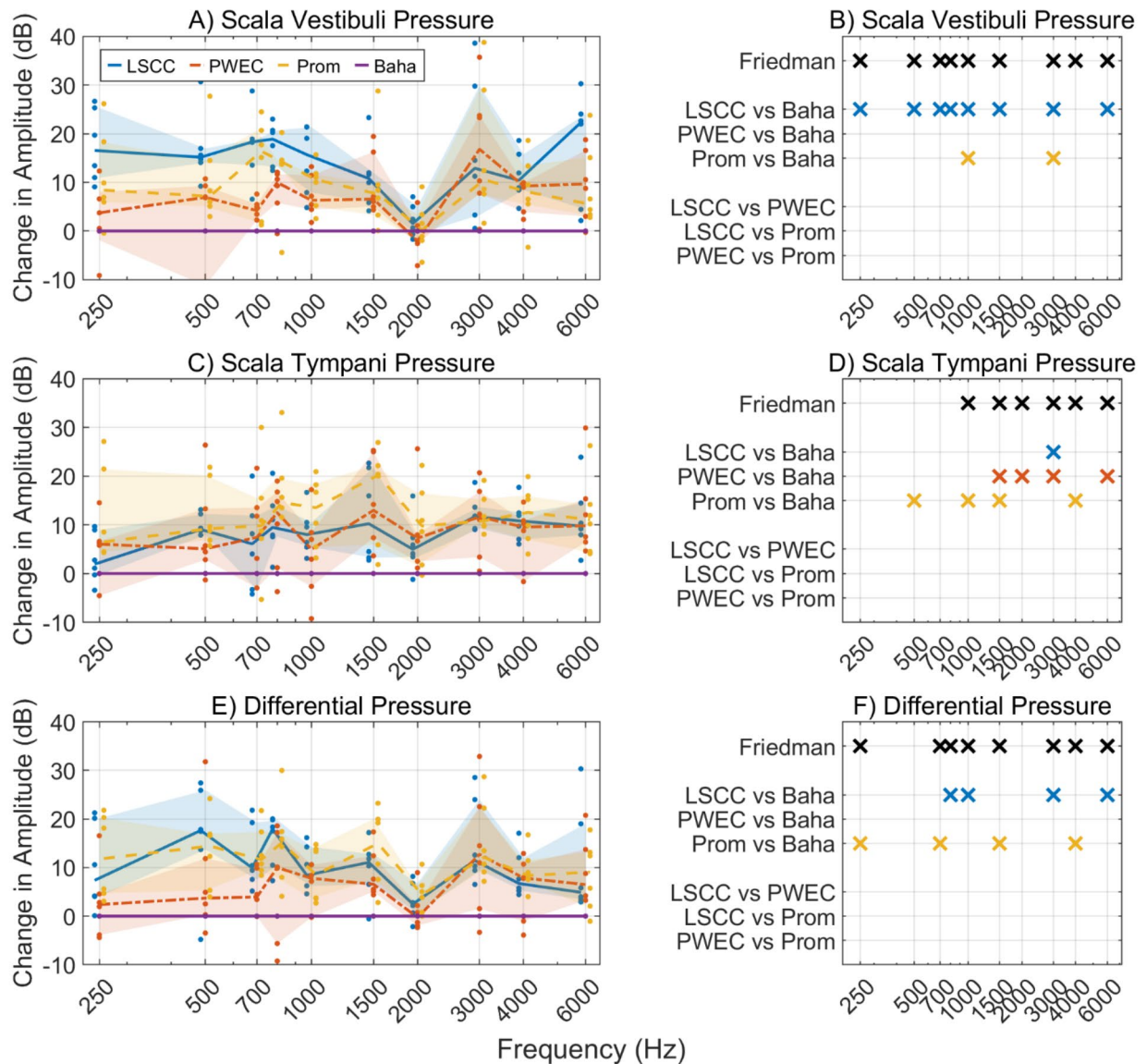


**Fig. 2.** Efficiency of the stimulation positions. (A,C,E) Change in amplitude when stimulating closer to the cochlea, compared to results from stimulating at the standard Baha position. Coloured lines represent the median across six individual ears, shaded areas represent the interquartile range, and dots show the results of individual specimens. (B,D,F) Indication of significant differences ( $p < 0.05$ ) between stimulating at different stimulation locations indicated by a cross (x), evaluated per frequency. From top to bottom: the Friedman test was used to identify differences across multiple stimulation positions. Additionally, a post-hoc Tukey-Kramer test on mean ranks was conducted to determine significant differences in pressures and velocities between stimulation positions. (A,B) Scala vestibuli pressure, (C,D) Scala tympani pressure, (E,F) Differential pressure.

is significant across all frequencies except 2 and 4 kHz when compared to stimulation at the standard Baha position. In contrast, stimulation at the promontory shows significant increases of approximately 10 dB at 1 and 3 kHz compared to the standard position. However, stimulation at the posterior wall of the ear canal does not result in significant differences relative to the standard Baha position. Additionally, no significant differences are observed when comparing stimulation among the three positions closer to the cochlea.

## Efficiency of stimulation positions

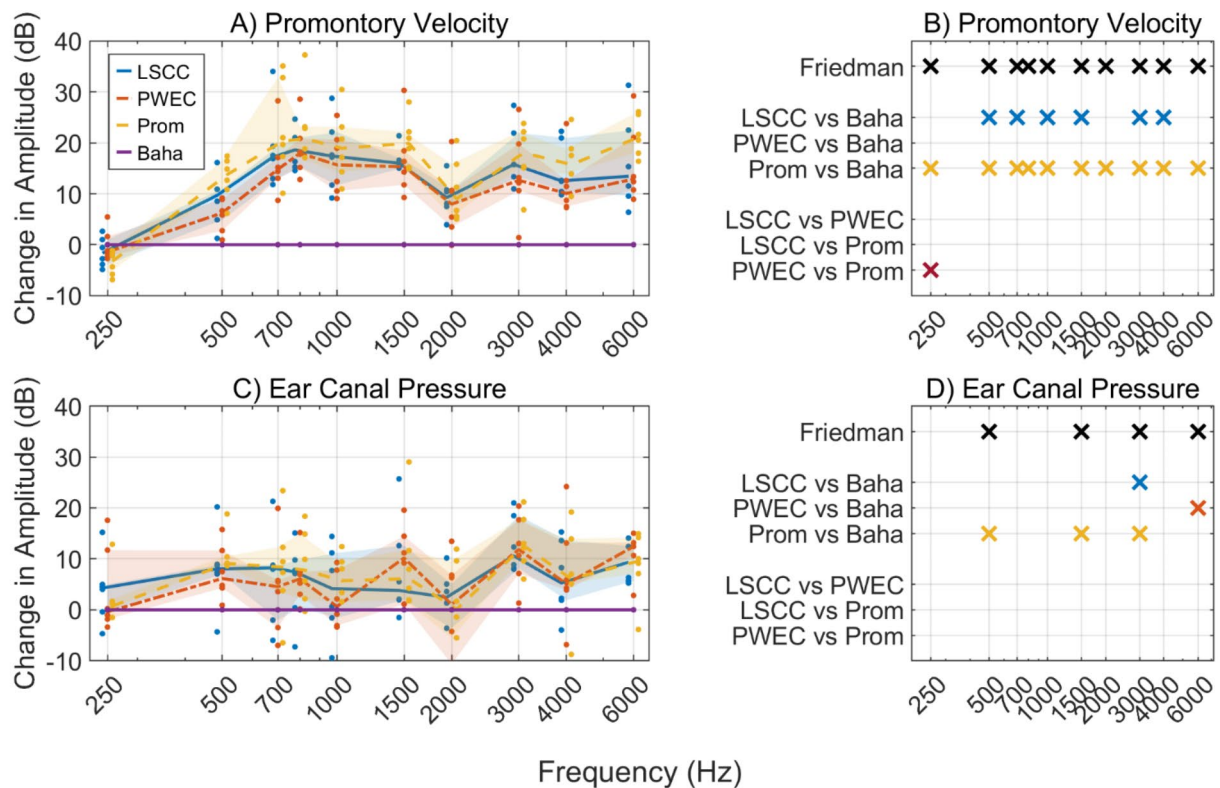


**Fig. 3.** Efficiency of the stimulation positions (part 2). (A,C) Change in amplitude when stimulating closer to the cochlea, compared to results from stimulating at the standard Baha position. Coloured lines represent the median across six individual ears, shaded areas represent the interquartile range, and dots show the results of individual specimens. (B,D) Indication of significant differences ( $p < 0.05$ ) between stimulating at different stimulation locations indicated by a cross (x), evaluated per frequency. From top to bottom: the Friedman test was used to identify differences across multiple stimulation positions. Additionally, a post-hoc Tukey-Kramer test on mean ranks was conducted to determine significant differences in pressures and velocities between stimulation positions. (A,B) Promontory velocity, (C,D) Ear canal pressure.

### Scala tympani pressure

Stimulation at the promontory yields the highest scala tympani pressures at 500, 1000, 1500, and 4000 Hz, with significant increases of 9, 14, 20, and 13 dB, respectively, compared to stimulation at the standard Baha position. Similarly, stimulation at the posterior wall of the ear canal results in significant pressure increases of 10 to 13 dB at 1.5, 2, 3, and 6 kHz compared to the Baha position. When stimulating at the lateral semi-circular canal, a significant increase of 12 dB is observed at 3 kHz compared to the Baha position. No significant differences, however, are observed when comparing stimulation among the three positions closer to the cochlea.

### Differential pressure

The differential pressure, defined as the complex difference between scala vestibuli and scala tympani pressures, shows significant increases when stimulating at the lateral semi-circular canal, with gains of 18, 8, 11, and 5 dB at 800, 1000, 3000, and 6000 Hz, respectively, compared to the standard Baha position. Stimulation at the promontory results in significant increases ranging from 8 to 12 dB at 250, 700, 1500, and 4000 Hz. In contrast, stimulation at the posterior wall of the ear canal does not yield significant differences compared to the standard Baha position, nor are there significant differences among the three positions closer to the cochlea.

### Promontory velocity

Stimulation at the promontory results in significant increases in promontory velocity, ranging from 9 to 21 dB across all frequencies except 250 Hz. At 250 Hz, however, a significant decrease of 2 to 3 dB is observed, not only in comparison to stimulation at the standard Baha position but also to the posterior wall of the ear canal. Similarly, stimulation at the lateral semi-circular canal leads to significantly increased velocities at 500, 700, 1000, 1500, 3000, and 4000 Hz. In contrast, stimulation at the posterior wall of the ear canal does not produce significantly increased velocities compared to the Baha position. Furthermore, aside from the decrease at 250 Hz, no significant differences are found among the positions closer to the cochlea.



### Ear canal pressure

Regarding ear canal pressure, significant increases are observed when stimulating at the lateral semi-circular canal at 3 kHz, at the posterior wall of the ear canal at 6 kHz, and at the promontory at 500, 1500, and 3000 Hz, compared to the standard Baha position.

### Correlation between measurement techniques

To assess the coherence among various measurement techniques, a principal component analysis is conducted. Figure 4 presents a scatterplot illustrating the responses obtained from the ear canal, promontory velocity, and differential pressure along with the best linear fit, while Table 1 summarizes the findings from these analyses. In addition, Supplementary Figs. S14 and S15, and Table S6 provide the results from the scala vestibuli and scala tympani pressure, while Supplementary Figs. S16–S30 and Supplementary Tables S7–S9 show the results for separate frequencies, specimens, and stimulation positions.

## Correlation between measurement techniques

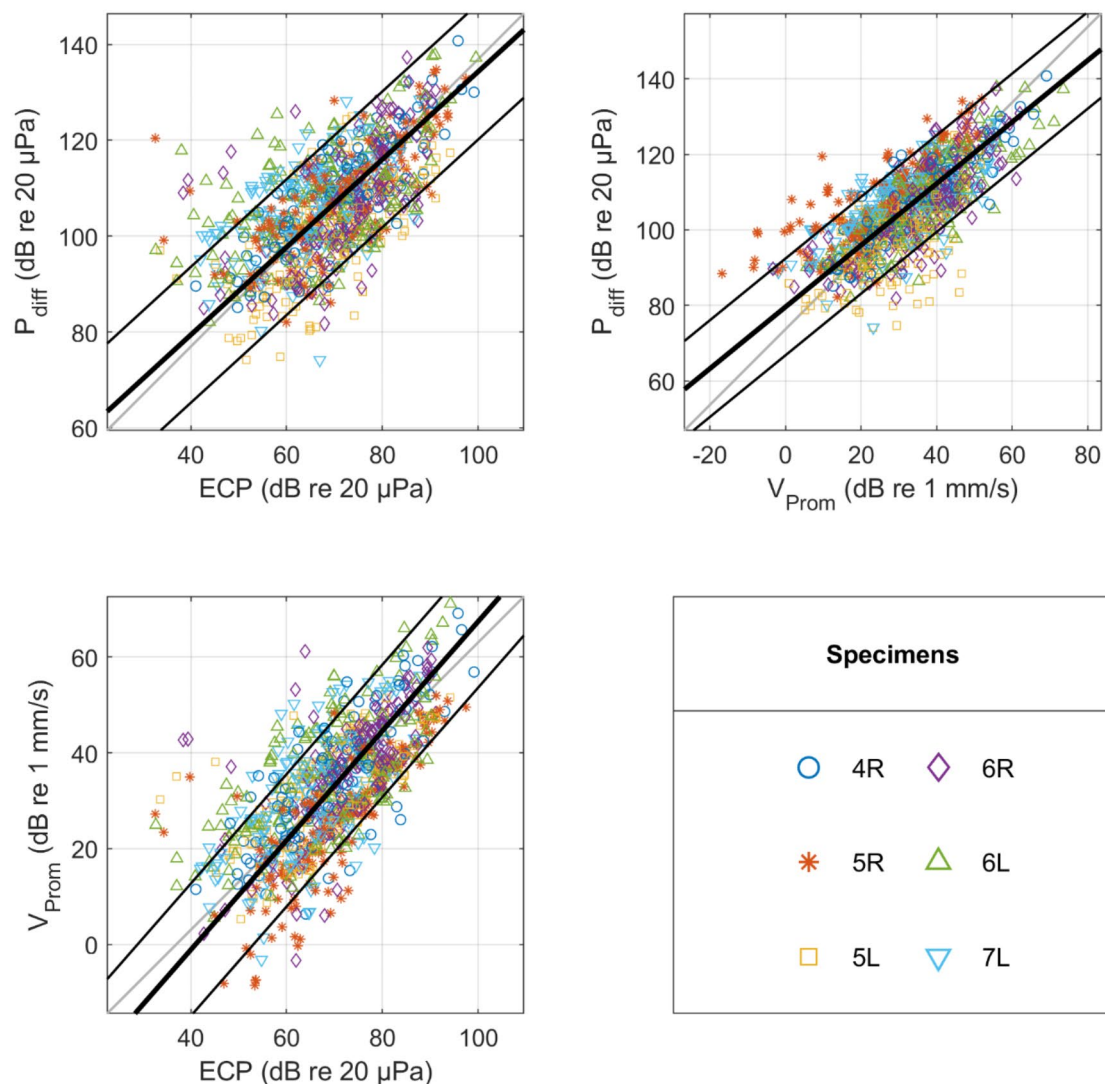


**Fig. 4.** Scatterplot of (A) the differential intracochlear pressure as a function of the ear canal pressure, (B) the differential intracochlear pressure as a function of the promontory velocity, and (C) the promontory velocity as a function of ear canal pressure. For the specimens, the number indicates the head and L and R are respectively the left and right side. The thick black line represents the best linear fit, with thin black lines demarcating the interquartile range. The grey line is a visual aid and represents a correlation with a slope of 1.

	Linear fit	Explained variance (%)	RMSE (dB)
$P_{diff}-ECP$	$P_{diff}=0.92 * ECP + 42.77 \text{ dB}$	80.6	7.23
$P_{diff}-V_{Prom}$	$P_{diff}=0.82 * V_{Prom} + 79.62 \text{ dB}$	85.9	6.53
$V_{Prom}-ECP$	$V_{Prom}=1.14 * ECP - 46.79 \text{ dB}$	83.8	7.04

**Table 1.** Characteristics of the principal component analysis between the differential pressure, the ear canal pressure, and the promontory velocity.

The linear fit indicates that the gains for predicting differential pressure based on ear canal pressure and promontory velocity are below unity, implying an overprediction of the differential pressure. This overprediction might be due to damping within the system. Moreover, ear canal pressure tends to underestimate promontory velocity. These discrepancies can also be explained since the different measurement techniques capture varying contributions from bone conduction pathways. Specifically, ear canal pressure reflects the contributions from ear canal compression and reverse stimulation from the middle ear, while promontory velocity accounts for the effects of cochlear inertia and compression. Differential pressure, on the other hand, captures contributions from as many as five bone conduction pathways. Furthermore, promontory velocity is measured in one dimension rather than three, which can lead to differences when compared with intracochlear pressure.

The best linear fit is found between the differential intracochlear pressure and the promontory velocity. However, even for these measures, the root mean square error between the data and the fit remains over 6 dB, which is larger than the test-retest variability observed in pure tone audiometry<sup>42</sup>. Consequently, ear canal pressure and promontory velocity cannot reliably predict intracochlear pressure, unless such an error of this magnitude is deemed acceptable for the specific interpretation or application.

When analysing the linear fit per frequency or specimen, some variability in the slope, intercept, explained variance, and RMSE was observed, but no clear trend emerged in this variability. However, separating the analysis by stimulation position revealed distinct patterns in the slopes. Specifically, slopes close to unity were observed for  $V_{Prom}$  as a function of ECP across all stimulation locations near the cochlea, indicating a nearly proportional relationship between ear canal pressure and promontory velocity. In contrast, at the standard Baha position, ECP underestimated  $V_{Prom}$ . Similarly, for  $P_{diff}$  relative to  $V_{Prom}$ , slopes close to unity were found for stimulation at the PWEC and promontory, suggesting a consistent transfer function between these variables at these locations. In contrast, for stimulation at the standard Baha position and LSCC,  $V_{Prom}$  tended to overestimate  $P_{diff}$ . Regarding  $P_{diff}$  as a function of ECP, the slope approached unity when stimulating at the promontory, indicating a proportional relationship. However, at the PWEC, ECP underestimated  $P_{diff}$  while at the standard Baha position and LSCC, ECP overestimated  $P_{diff}$ .

Effect of occlusion

Since the measurements are performed with an occluded ear canal, but in clinical practice, patients will have an open ear canal, the effect of occlusion was also investigated in a subgroup. Figure 5 shows the difference in intracochlear pressure, and promontory velocity with and without ear tip when stimulating at the promontory. While individual results vary, the 95% confidence interval includes 0 dB for each frequency, except for the scala vestibuli pressure at 1 kHz., which could be a false positive.

Control measurements

Control measurements were performed to assess whether the specimen was representative of a normal hearing person, whether air bubbles appeared in the cochlea due to the preservation, leading to alterations in the mechanical properties, and whether the signal of the intracochlear pressures remained stable throughout the whole experiment. Results are shown in Supplementary Figs. S1–S8, resulting in the exclusion of specimens 1 L, 2R, 3 L, 3R, and 4 L.

Discussion

The main constraint of current BCIs is the maximum output force level, resulting in a fitting range of pure tone BC averages of up to 45 dB for most transcutaneous devices<sup>6–9</sup>. This experimental study evaluated the stimulation of three surgically accessible positions closer to the cochlea: the lateral semi-circular canal, the posterior wall of the ear canal, and the promontory. To investigate whether stimulating at these positions resulted in more efficient sound transfer, three objective measures were recorded simultaneously: intracochlear pressure, promontory velocity, and ear canal pressure.

As hypothesized, results show that stimulating closer to the cochlea, i.e., at the lateral semi-circular canal, promontory, or posterior wall of the ear canal, generates higher responses for the different objective measures. Regarding promontory movement, when stimulating at the lateral semi-circular canal, the results align with the ones of Niemczyk et al.<sup>15</sup>, showing an increased response when stimulating closer to the cochlea, especially above 1 kHz. In addition, these findings support those of Verhaert et al.<sup>17</sup>, who demonstrated that the lateral semi-circular canal is a viable site for stimulation, based on 1D LDV measurements of stapes velocity. The results also align with those of Felix et al.<sup>43</sup> with increased promontory velocity and scala vestibuli and tympani pressure when stimulating at the lateral semi-circular canal and the stylomastoid foramen.

Moreover, a consistent dip in gain relative to stimulation at the Baha position was observed around 2 kHz. This dip can be explained by the mechanical impedance characteristics of the skull, which relate to the force applied relative to the resulting velocity at the skull surface, and the cochlear promontory. As described by

## Occlusion effect

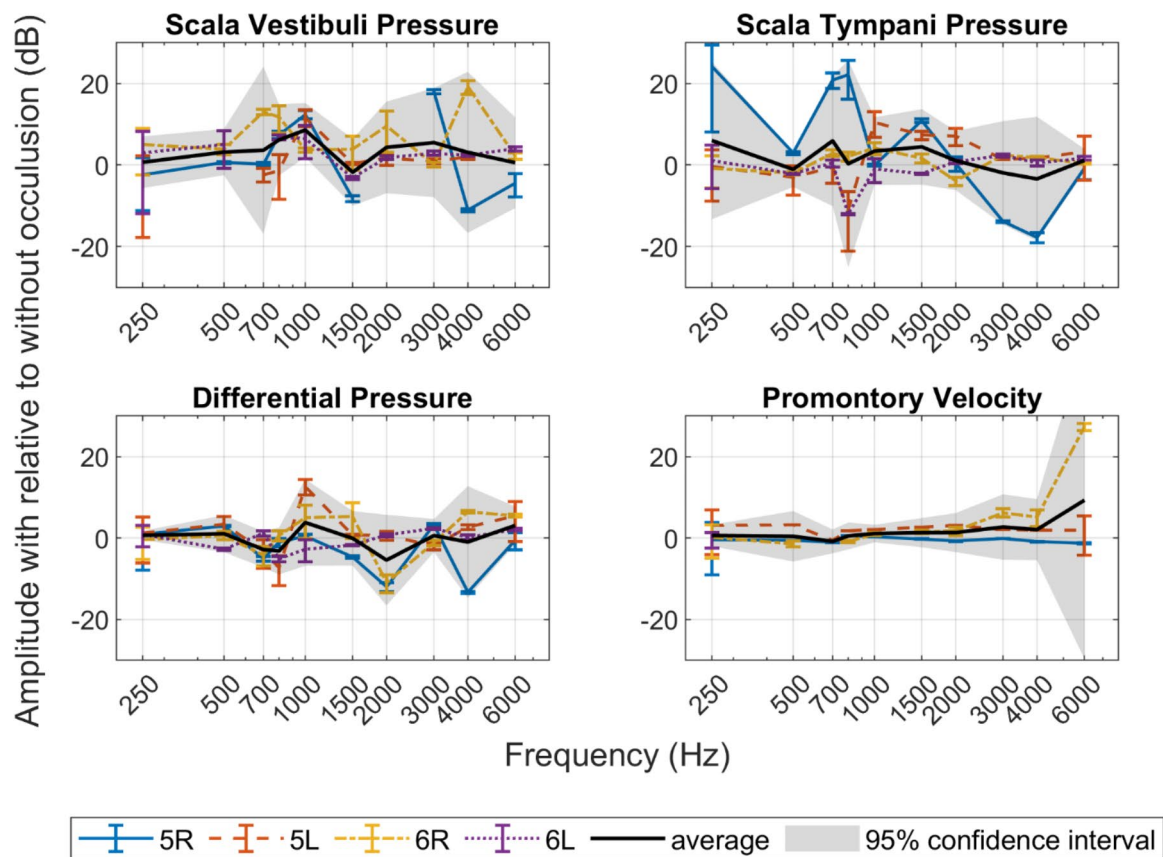


**Fig. 5.** The difference in intracochlear pressure and promontory velocity amplitude, with and without ear tip in the ear canal during bone conduction stimulation at the promontory. For the specimens, the number indicates the head and L and R are respectively the left and right side.

Stenfelt and Goode<sup>16</sup> and Håkansson<sup>44</sup>, mechanical impedance is frequency-dependent, with lower impedance values around 2 kHz indicating reduced resistance to the propagation of vibrational energy through the skull. Consequently, at this frequency, the force applied at the Baha position effectively drives skull vibrations, leading to relatively efficient sound transfer to the inner ear. This efficient transfer leaves little room for further improvement when stimulating closer to the cochlea.

Furthermore, the results show discrepancies between the different measurement techniques, which is confirmed by the correlation analysis. These discrepancies can be explained by the fact that the three measurement techniques incorporate varying aspects of the BC pathways and the stimulation position might change the contributions of these pathways, as confirmed by the principal component analysis per stimulation position. In addition, velocity is a vector unit and is measured here in only one dimension as opposed to 3 component experiments performed by Dobrev et al.<sup>35,45</sup>. Thus, measurements of the promontory velocity will inherently have a margin of error. A downside of the pressure sensors is that they might pick up artefacts due to relative motion between the sensor and the cochlea, especially when stimulating close to the cochlea. However, both Felix et al.<sup>43</sup> and Borgers et al.<sup>21</sup> proved that fixating the sensor to the cochlea greatly reduces these artefacts, making their contribution negligible.

The differential intracochlear pressure is the measurement technique closest to the organ of Corti, includes the contributions of all five BC pathways, and provides a scalar response. Additionally, Putzeys et al.<sup>24</sup> demonstrated that the perceived loudness of air and bone conduction sound during psychoacoustic tests validates intracochlear pressure as an objective indicator of the cochlear drive. Therefore, we assume that this technique is the most accurate for objective evaluation of the hearing sensation. Our findings conclude that stimulation at the lateral semi-circular canal or promontory results in the most efficient sound transfer and thus a broader fitting range. Furthermore, this study is the first to investigate stimulation close to the cochlea, with three objective measures – intracochlear pressure, promontory velocity, and ear canal pressure – simultaneously, thus providing baseline data that can be invaluable for future research in the field.

This improved fitting range is especially relevant for patients necessitating output force levels surpassing the current maximum. However, achieving stimulation closer to the cochlea requires a surgical opening for access, resulting in a more invasive procedure compared to the placement of a BCI on the skull surface. Nonetheless, in scenarios such as electro-vibrational stimulation<sup>18</sup>, where a cochlear implant is also utilized, the surgical opening required for this procedure is readily available.

In addition to the benefits observed in the current study, previous research<sup>16,46,47</sup> has shown that stimulating closer to the cochlea can reduce transcranial transmission or the relative hearing between the contralateral and ipsilateral side. While our study did not measure the contralateral side to directly assess this effect, this reduction in crossover can improve the separation between the sounds perceived by the ipsilateral (same side) and contralateral (opposite side) ears, thereby enhancing the patient's ability to localize sounds.

One of the main limitations of this study is that stimulation was conducted on specimens without any pathology leading to conductive hearing loss. Given the targeted application of BCIs toward mitigating this auditory impairment, a critical avenue for further investigation involves assessing the efficacy of stimulation on specimens afflicted with conductive hearing loss. These pathologies include tympanic membrane perforation, otosclerosis, round window reinforcement, and superior canal dehiscence. The effect of these pathologies on air conduction and bone conduction stimulation at the skull surface is already studied both with preclinical tests<sup>27,48,49</sup> in cadaveric specimens as well as with computer models<sup>3,50–56</sup>.

Furthermore, the angle between the direction of stimulation and the surface of the stimulated bone was intended to remain consistent across all measurements. Variations in this angle could affect the results, introducing additional variation between specimens in the three objective measures. More pronounced quantitative changes to the stimulation angle could provide deeper insights into bone conduction (BC) stimulation mechanisms. However, due to the constraint of the support structure from the shaker, only limited adjustment to this angle was possible. Consequently, measurements with significant angle changes were not conducted.

Additionally, the ear tip remained in the ear canal during all measurements to ensure consistent ear canal pressure and repeatable air conduction measurements. Therefore, all results should be interpreted in the context of an occluded ear canal. While stimulating at the skull surface typically produces an occlusion effect<sup>57</sup>, we did not detect a significant effect on the occluded ear when stimulating at the cochlear promontory.

Lastly, the shaker setup relies on static pre-load to maintain contact between the driver and the skull. While this method allows for effective force transmission, it is more similar to non-implantable devices, such as the Cochlear BAHA Softband or Radioear B-81, which also use contact pressure than to implantable devices, which use direct bone anchorage.

## Conclusion

This study shows that bone conduction stimulation closer to the cochlea results in up to 20 dB higher intracochlear pressure. Since intracochlear pressure is a predictor of hearing sensation, this could increase the efficacy of the BC devices. These results are particularly interesting for patients requiring higher than the current maximum output force levels, for patients eligible for electro-vibrational stimulation, and for the development of new BC implants.

## Methods

### Test setup

The experimental setup follows our previous studies and aligns with other research on intracochlear pressure measurement during both air conduction (AC) and bone conduction (BC) stimulation. Fresh-frozen human cadaveric specimens were obtained from the Vesalius Institute (Anatomy and Pathology, University of Leuven - KU Leuven, Belgium), with ethical approval from the Medical Ethics Committee of the University Hospitals of Leuven (S65502) following the Helsinki Declaration. Donors gave informed consent during their lifetime. Our harvesting and preparation procedures were consistent with our prior work<sup>21,23–25</sup> and established methods in intracochlear pressure measurement from literature<sup>20,22,29,58,59</sup>.

### Specimens

The specimens, harvested within 72 h post-mortem according to ASTM-F2504 guidelines<sup>38</sup>, were frozen at  $-20\text{ }^{\circ}\text{C}$  and thawed at  $2\text{ }^{\circ}\text{C}$  48–72 h before experimentation. Surgical preparation involved a canal-wall-up mastoidectomy with enlarged posterior tympanotomy, including removing the mastoid portion of the facial nerve, delicate drilling of the anterior and posterior pillars of the round window niche to enhance the visibility of the round window membrane, and removing any obstructing pseudo membranes. The cochlear wall was thinned at the base of the scala vestibuli (SV) and scala tympani (ST) for intracochlear pressure sensor insertion. Throughout the experiments, except for specimens 1, 2, and 7, both ears of every full-head specimen were measured (indicated with xR or xL throughout the text). Following surgical preparation, each specimen was placed on its side with a ring of modelling clay (Play-Doh, Hasbro, Pawtucket, USA) encircling the contralateral ear to prevent direct contact with the vibration-isolation table (M-VIS3048-SG2-325 A, Newport Spectra-Physics, the Netherlands). The donor's age ranged from 67 to 93 years old. Three out of seven donors were female.

### Stimulation

An insert earphone (ER-3 C, Etymotic Research, Illinois, USA) was used to assess the specimens' representativeness for healthy human ears with air conduction. The foam tip of the insert earphone was gently inserted into the ear canal and remained in position throughout the experiment, including bone conduction stimulation, to ensure consistency and minimize variability from repeated placements. At the conclusion of the experiment, the foam tip was removed, and one additional measurement was conducted to assess the impact of occlusion.



Bone conduction stimulation was conducted using an experimental setup comprising a shaker (Type 4810, Brüel & Kjær, Denmark), and a custom-made rod, depicted in Fig. 6A. To establish stable contact between the skull and the rod end tip (0.8 mm diameter), a small pit was drilled into the skull cortex bone using a 1 mm drill. After the initial contact, the shaker was advanced an additional 500  $\mu\text{m}$  to firmly press the rod against the skull. This pressure provides a static pre-load, which ensures that the rod maintains contact with the skull even during the negative phase of the waveform. This configuration allows the setup to simulate both compressive and tensile forces, offering a more complete approximation of the behaviour of bone-anchored hearing devices. However, it is important to note that this setup is still more comparable to non-implantable devices, such as the Cochlear BAHA Softband or Radioear B-81, which similarly rely on contact pressure rather than direct bone anchorage. The rod was in contact with the specimen at four different positions: the standard Baha position<sup>41</sup>, the lateral semi-circular canal, the posterior wall of the ear canal, and the promontory as shown in Fig. 1. Figure 6B and C illustrate the angle between the rod and the specimen. Angle  $\alpha$  varied between 64° and 86°, for all specimens and stimulation positions, while angle  $\beta$  varied between 58° and 90°.

Matlab (2018b Mathworks, Massachusetts, USA) was employed to generate signals, which were then delivered to the insert phone and shaker via a sound card (Fireface UC, RME, Haimhausen, Germany) and an amplifier set to a unit gain (AC: LPA01, Newtons4th Ltd., Leicester, UK; BC: Type 2718, Brüel & Kjær, Denmark).

Two types of signals were utilized: a stepped sine wave ranging from 100 Hz to 10 kHz with 50 logarithmically spaced frequencies at a stimulation voltage of 0.2 V RMS, repeated ten times per measurement, and a single-frequency sine signal lasting 50s. For the latter, ten frequencies were used: 250 Hz, 500 Hz, 700 Hz, 800 Hz, 1 kHz, 1.5 kHz, 2 kHz, 3 kHz, 4 kHz, and 6 kHz. Due to a 750 Hz noise source in the measurement chamber, the frequency conventionally used in this type of experiment was substituted with 700 and 800 Hz.

### Measurements

In addition to the insert earphone, a probe tube microphone (ER-7 C, Etymotic Research, USA) was integrated into the insert phone plug within the ear canal to measure the ear canal pressure. The recording was performed with the same sound card as the stimulation. The output force level (OFL) applied by the shaker was measured by an impedance head (Type 8001, Brüel & Kjær, Denmark).

Velocity measurements of the posterior crus of the stapes, the round window membrane, and the promontory were conducted using a single-point laser 1D Doppler vibrometry system mounted on a surgical microscope (OFV-534 Compact Sensor Head and A-HLV MM 30 Micromanipulator; OFV-5000 Vibrometer controller; Polytec GmbH, Waldbronn, Germany). A laser beam targeted a 500  $\times$  500  $\mu\text{m}^2$  piece of retroreflective tape (A-RET-T010, Polytec GmbH, Waldbronn, Germany) on these structures, positioned normally to their surfaces. Output from the laser Doppler vibrometry system was recorded by an external sound card (Fireface UC, RME, Haimhausen, Germany) during stepped sine wave stimulation, while data acquisition during single frequency sine wave stimulation was performed using a lock-in amplifier (SR830, Stanford Research Systems, Sunnyvale, CA, USA).

Pressure measurements in both scala vestibuli and tympani were concurrently conducted using two commercial fibre-optic pressure sensors (FOP M-260, FISO Technologies, Canada) with an outer diameter of approximately 310  $\mu\text{m}$ . An interferometer (OCT Common-Path Interferometer, Thorlabs, Germany) converted the sensors' optical signals to electrical signals using a low-coherent infrared light source (S5FC1021S - SM Benchtop SLD Source, 1310 nm, 12.5 mW, 85 nm Bandwidth, Thorlabs, Germany). Signal demodulation is typically used to determine the precise position of the pressure sensor membrane, but here, emphasis was placed on the sine wave's amplitude. Calibration, performed in a vibrating water column as described by Piffner et al.<sup>60</sup> and Borgers et al.<sup>21</sup>, established a linear conversion ratio between the sensor-generated potential and the

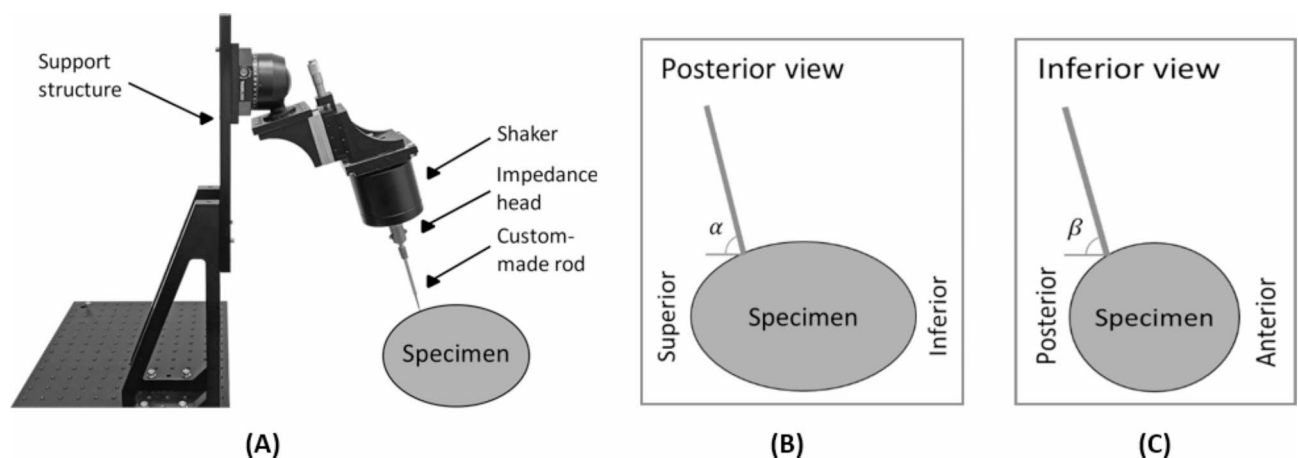


**Fig. 6.** (A) Illustration of the experimental setup, including a support structure, a shaker for stimulation, an impedance head for measuring output force, and a custom-made rod for specimen contact. (B) Posterior view and angle ( $\alpha$ ), and (C) Inferior view and angle ( $\beta$ ) of the connection between the rod and the specimen.

pressure wave's amplitude. Data acquisition was performed using a lock-in amplifier (SR830, Stanford Research Systems, USA) to address the low signal-to-noise ratio.

## Experimental procedure

### *Middle and inner ear transfer function*

The middle ear transfer function (METF), representing the ratio of stapes velocity to ear canal pressure, was measured both before and after sensor insertion. To obtain this measure the insert earphone was stimulated with the stepped sine wave at 0.2 V RMS. The results are compared with the range delineated by Koch et al.<sup>61</sup>, providing insight into the specimen's representativeness within the population, though this range does not serve as an exclusion criterion. Additionally, evaluating significant differences between pre- and post-sensor insertion measurements enables examination of mechanical changes resulting from the drilling and insertion process. Significance was assessed using a paired t-test ( $\alpha = 0.05$ ), with a false discovery rate correction applied for multiple comparisons ( $n = 500$ , covering 50 frequencies across ten specimens).

Furthermore, the velocity of the round window, measured equivalent to the stapes velocity, was analysed. The expected phase difference between the stapes and round window velocity is  $180^\circ$ , assuming the cochlear fluid's incompressibility and the round and oval windows as the primary fluid outlets<sup>62,63</sup>. This measurement serves as an additional control measure. Deviations from the expected  $180^\circ$  may suggest various factors, including the presence of a compressible air bubble in the cochlea, reinforcement of one of the fluid outlets, or the emergence of an additional outlet.

### *Sensor insertion*

Sensor insertion began by immersing the middle ear in saline to safeguard against air ingress into the cochlea. Utilizing a 0.5 mm diamond burr and a 0.35 mm perforator, a cochleostomy was drilled in the scala vestibuli. Next, employing a micromanipulator (MD4, Märzhäuser Wetzlar GmbH & Co.KG, Germany), the sensor was cautiously inserted approximately 100–300  $\mu\text{m}$  into the scalae. Subsequently, the sensor was sealed with dental impression material (Alginoplast<sup>®</sup>, Heraeus Kulzer GmbH, Germany). After partial saline removal, the sensor was affixed using bone cement (Durelon, 3 M, USA) to prevent relative motion between the sensor and the cochlea. This procedure was replicated for the scala tympani. Following cementation, each sensor was released from the micromanipulators to minimize artificial pressure<sup>21</sup>. Throughout this process, a stimulus of 90 dB re 20  $\mu\text{Pa}$  at 1 kHz was directed to the insert phone, and the pressure sensor's output was scrutinized in real-time to ensure it remained clear of the cochlear wall.

### *Noise measurement*

To minimize the influence of non-random noise during measurements, a 'dark' or 'silent' measurement was performed before the stimulation experiments. By subtracting the complex difference between the stimulation measurements and this silent baseline, we corrected any correlated noise captured by the lock-in amplifier<sup>24,64</sup>.

### *Measurements with bone conduction stimulation close to the cochlea*

For these measurements, the tip of the rod from the shaker was positioned at four locations: the standard Baha position, the lateral semi-circular canal, the posterior wall of the ear canal, or the promontory. The shaker stimulated the specimen with single-frequency sine signals. Intensities at the standard Baha location were adjusted individually for each ear to achieve a differential pressure of 100 dB re 20  $\mu\text{Pa}$  between the scalae; at other locations, stimulation levels were calibrated to achieve the same output force level as at the standard Baha position. The resulting output force levels are shown in Fig. 7. Additionally, bone conduction measurements were repeated with the shaker's output potential varied by  $\pm 10$  dB. Ear canal pressure and output force levels were recorded using a sound card, while promontory velocity and intracochlear pressures were measured with lock-in amplifiers.

During shaker repositioning, a 90 dB re 20  $\mu\text{Pa}$  stimulus at 1 kHz was applied to the insert phone, with real-time monitoring of the probe microphone and intracochlear sensor output to ensure signal integrity. In addition, the air conduction response at 0.25, 0.5, 1, 2, and 4 kHz was measured when stimulating the insert earphone at 90 dB HL. Normalization of intracochlear pressures to ear canal pressure facilitated comparison with existing literature<sup>59,65–67</sup>, providing insight into specimen representativeness. Moreover, it served to confirm sensor stability throughout the experiment.

## Analysis

### *Preprocessing*

The recorded potential values were converted to pressure in Pa, velocity in mm/s, and force in N as part of the processing with Matlab. The differential pressure was then derived as the complex difference between SV and ST pressure, obtained simultaneously by individual lock-in amplifiers. An iterative procedure corrected for rise and fall time, detecting and removing data samples deviating more than two times the standard deviation from the mean within the initial and final 8 s. This adjustment aimed to mitigate the effect of computer lag and lock-in amplifier integration time.

Subsequently, detrending using the 'detrend' function in Matlab eliminated signal drift. Stimulation measurements were compared to dark measurements to determine noise interference by calculating the mean and standard deviation for both in the complex domain. These values formed ellipses in the complex plane, with major and minor axes corresponding to the standard deviation of the real and imaginary parts. If the ellipses intersected, indicating indistinguishable noise, we excluded the data from further analysis. Otherwise, we calculated mean amplitude and phase, along with variance using linear perturbation theory based on Taylor expansion<sup>68</sup>.

## Output Force Level

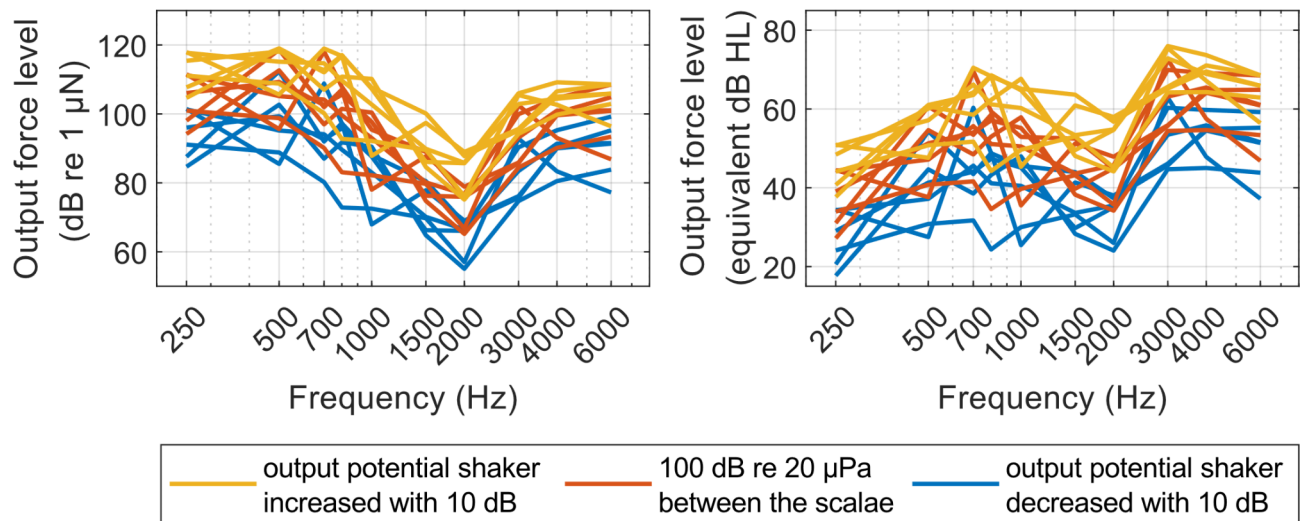


**Fig. 7.** Output force levels during bone conduction stimulation. Colours represent the different stimulation levels. Individual lines represent individual ears. On the left side, the level is shown relative to 1 µN. On the right side, it is shown as the equivalent level in dB hearing level, obtained by subtracting the relative equivalent threshold vibratory force level.

### Efficiency of stimulation positions

To enable easy comparison between the responses of the intracochlear pressure, promontory velocity, and ear canal pressure, the increase relative to stimulation at the standard Baha position is calculated. First, the absolute amplitudes (abs) of these measurements are divided by the corresponding output force level (OFL). Thereafter, the results are converted to decibels and lastly, the difference of the amplitudes for stimulation at a position closer to the cochlea (pos ii, where ii is an integer corresponding to the stimulation site number) and at the standard Baha position (pos ii = Baha) is calculated. Thus, the pressure (P) increase (incr) is calculated as follows:

$$P_{incr}^{pos\ ii} (dB) = 20 \cdot \log_{10} \left( \frac{P_{abs}^{pos\ ii} (Pa)}{OFL_{abs}^{pos\ ii} (N)} \right) - 20 \cdot \log_{10} \left( \frac{P_{abs}^{Baha} (Pa)}{OFL_{abs}^{Baha} (N)} \right) \quad (1)$$

The data underwent normality testing using the Shapiro-Wilk test, but due to the small sample size, a normal distribution was not assured. Consequently, the Friedman test was used to identify differences across multiple stimulation positions. Additionally, a post-hoc Tukey-Kramer test on mean ranks was conducted to determine significant differences in pressures and velocities between stimulation positions.

### Correlation between measurement techniques

To evaluate the predictive capacity of various measurement techniques, principal component analysis (PCA) was employed to obtain the best linear fit between each pair of measurements. The slope of the best-fit line was determined by the ratio of the elements of the first principal component, while the intercept was computed to ensure that the fit passed through the mean of the data. Additionally, the percentage of the total variance explained by the first principal component was reported. Finally, the root mean square error (RMSE) was calculated by taking the square root of the average squared residuals, representing the deviation of the data points from the best-fit line along the direction of the second principal component. Each measurement at each frequency, in each individual ear, at each stimulation position, and intensity was considered an independent observation, since they were applied sequentially and recorded with a lock-in amplifier independent of each other.

### Occlusion effect

At the conclusion of the experiment, the foam tip from the insert earphone was removed, and one additional bone conduction measurement was conducted to assess the impact of occlusion. The difference between the intracochlear pressures, and promontory velocity was calculated and a t-test was performed to assess whether the effect was significant.

### Data availability

All data analysed during this study are included in this published article. The full datasets can be provided by Nicolas Verhaert (nicolas.verhaert@kuleuven.be) upon reasonable request.

Received: 4 July 2024; Accepted: 27 November 2024

Published online: 02 December 2024

## References

- Ellsperman, S. E., Nairn, E. M. & Stucken, E. Z. Review of bone conduction hearing devices. *Audiol. Res.* **11**, 207–219 (2021).
- WHO. *World report on hearing*. World Health Organization (2021). <https://apps.who.int/iris/handle/10665/339913> %0Alicencia: CC BY-NC-SA 3.0 IGO.
- Stenfelt, S. Investigation of mechanisms in Bone Conduction Hyperacusis with Third Window pathologies based on model predictions. *Front. Neurol.* **11**, 966 (2020).
- Tsai, V., Ostroff, J., Korman, M. & Chen, J. M. Bone-conduction hearing and the occlusion effect in otosclerosis and normal controls. *Otol Neurotol.* **26**, 1138–1142 (2005).
- Chhan, D., Rösli, C., McKinnon, M. L. & Rosowski, J. J. Evidence of inner ear contribution in bone conduction in chinchilla. *Hear. Res.* **301**, 66–71 (2013).
- Arndt, S. et al. Vorhersage Des Postoperativen Sprachverstehens Mit dem transkutanen teilimplantierbaren Knochenleitungshörsystem Osia. *HNO* **72**, 1–9 (2024).
- Zernotti, M. E. & Sarasty, A. B. Active bone conduction prosthesis: BonebridgeTM. *Int. Arch. Otorhinolaryngol.* **19**, 343–348 (2014).
- Pla-Gil, I. et al. Clinical performance Assessment of a new active Osseointegrated Implant System in mixed hearing loss: results from a prospective clinical investigation. *Otol Neurotol.* **42**, E905–E910 (2021).
- Verhaert, N., Desloovere, C. & Wouters, J. Acoustic hearing implants for mixed hearing loss. *Otol Neurotol.* **34**, 1201–1209 (2013).
- Ghossaini, S. N. & Ying, Y. M. Management of Conductive hearing loss with Implantable Bone Conduction devices. *Oper. Tech. Otolaryngol. - Head Neck Surg.* <https://doi.org/10.1016/j.otot.2024.01.011> (2024).
- Maier, H. et al. Consensus Statement on Bone Conduction Devices and active middle ear implants in conductive and mixed hearing loss. *Otol Neurotol.* **43**, 513–529 (2022).
- Hua, H., Goossens, T. & Lewis, A. T. Increased maximum power output may improve speech recognition with bone conduction hearing devices. *Int. J. Audiol.* **61**, 670–677 (2022).
- Bergius, E., Philipsson, M., Rosenbom, T. & Sadeghi, A. Benefit of higher Maximum Force output in bone anchored hearing systems: a crossover study. *Otol Neurotol.* **42**, 1451–1459 (2021).
- Eeg-Olofsson, M., Stenfelt, S., Tjellstrom, A. & Granstrom, G. Transmission of bone-conducted sound in the human skull measured by cochlear vibrations. *Int. J. Audiol.* **47**, 761–769 (2008).
- Niemczyk, K. et al. Effectiveness of bone conduction Stimulation Applied directly to the Otic Capsule measured at Promontory: Assessment in Cadavers. *Audiol. Neurotol.* **25**, 143–150 (2020).
- Stenfelt, S. & Goode, R. L. Transmission properties of bone conducted sound: measurements in cadaver heads. *J. Acoust. Soc. Am.* **118**, 2373–2391 (2005).
- Verhaert, N., Walraevens, J., Desloovere, C., Wouters, J. & Gérard, J. M. Direct acoustic stimulation at the lateral canal: an alternative route to the inner ear? *PLoS One.* **11**, 1–17 (2016).
- Geardyn, A., De Voedt, K., Wouters, J. & Verhaert, N. Electro-vibrational stimulation results in improved speech perception in noise for cochlear implant users with bilateral residual hearing. *Sci. Rep.* **13**, 1–9 (2023).
- American Society for Testing and Materials. *ASTM F2504-05(2014) Standard Practice for Describing System Output of Implantable Middle Ear Hearing Devices*. (2014). <https://doi.org/10.1520/f2504-05r14> doi:10.1520/F2504-05R14.
- Greene, N. T. et al. Cochlear implant electrode effect on sound energy transfer within the cochlea during acoustic stimulation. *Otol Neurotol.* **36**, 1554–1561 (2015).
- Borgers, C., Fierens, G., Putzeys, T., van Wieringen, A. & Verhaert, N. Reducing artifacts in Intracochlear pressure measurements to Study Sound transmission by bone conduction stimulation in humans. *Otol Neurotol.* **40**, e858–e867 (2019).
- Mattingly, J. K. et al. A comparison of Intracochlear pressures during Ipsilateral and Contralateral Stimulation with a bone conduction Implant. *Ear Hear.* **41**, 312–322 (2020).
- Fierens, G. et al. The Impact of Location and Device Coupling on the Performance of the Osia System Actuator. *Biomed Res. Int.* **1–16** (2022). (2022).
- Putzeys, T. et al. Intracochlear pressure as an objective measure for perceived loudness with bone conduction implants. *Hear. Res.* **422**, 108550 (2022).
- Wils, I. et al. Objective preclinical measures for bone conduction implants. *Front. Neurosci.* **18**, (2024).
- Dancer, A. & Franke, R. Intracochlear sound pressure measurements in guinea pigs. *Hear. Res.* **2**, 191–205 (1980).
- Nielsen, M. E. F. et al. Assessment of the effects of Superior Canal Dehiscence Location and size on Intracochlear Sound pressures. *Audiol. Neurotol.* **20**, 62–71 (2015).
- Guan, X., Cheng, Y. S., Galaiya, D. & Nakajima, H. H. American Institute of Physics Inc., The effect of round window reinforcement on human hearing. In *13th Mechanics of Hearing Workshop: To the Ear and Back Again - Advances in Auditory Biophysics*, MoH 2017 (eds. C., B. & S., P.) vol. 1965 150004 (2018).
- Stieger, C. et al. Intracochlear Sound pressure measurements in normal human temporal bones during Bone Conduction Stimulation. *J. Assoc. Res. Otolaryngol.* **19**, 523–539 (2018).
- Rosowski, J. J., Chien, W., Ravicz, M. E. & Merchant, S. N. Testing a method for quantifying the output of Implantable Middle ear hearing devices. *Audiol. Neurotol.* **12**, 265–276 (2007).
- Roosli, C. et al. Intracranial pressure and Promontory Vibration with Soft tissue stimulation in Cadaveric Human whole heads. *Otol Neurotol.* **37**, e384–e390 (2016).
- Rigato, C. et al. Effect of transducer attachment on vibration transmission and transcranial attenuation for direct drive bone conduction stimulation. *Hear. Res.* **381**, (2019).
- Prodanovic, S. & Stenfelt, S. Review of whole Head Experimental Cochlear Promontory vibration with Bone Conduction Stimulation and Investigation of Experimental Setup effects. *Trends Hear.* **25**, 233121652110527 (2021).
- Ghoncheh, M. et al. Output performance of the novel active transcutaneous bone conduction implant Sentio at different stimulation sites. *Hear. Res.* **108369** <https://doi.org/10.1016/j.heares.2021.108369> (2021).
- Dobrev, I. et al. Influence of stimulation position on the sensitivity for bone conduction hearing aids without skin penetration. *Int. J. Audiol.* **55**, 439–446 (2016).
- Dobrev, I., Pfiffner, F. & Rösli, C. Intracochlear pressure and temporal bone motion interaction under bone conduction stimulation. *Hear. Res.* **435**, 108818 (2023).
- Dobrev, I., Farahmandi, T. S. & Rösli, C. Experimental investigation of the effect of middle ear in bone conduction. *Hear. Res.* **395**, (2020).
- ASTM. *F2504-05 Standard Practice for Describing System Output of Implantable Middle Ear Hearing Devices*. <https://www.astm.org/f2504-05r22.html> (2022).
- Nie, Y. et al. An objective bone conduction verification tool using a piezoelectric thin-film force transducer. *Front. Neurosci.* **16**, 1–18 (2022).
- Mertens, G., Desmet, J., Snik, A. F. M. & Van De Heyning, P. An experimental objective method to determine maximum output and dynamic range of an active bone conduction implant: the Bonebridge. *Otol Neurotol.* **35**, 1126–1130 (2014).



41. Cochlear Limited. Cochlear TM Osia<sup>®</sup> OSI200 Implant Physician's Guide. (2019).
42. Jerlval, L., Dryselius, H. & Arlinger, S. Comparison of manual and computer-controlled audiometry using identical procedures. *Scand. Audiol.* **12**, 209–213 (1983).
43. Felix, T. R. et al. Estimating vibration artifacts in preclinical experimental assessment of actuator efficiency in bone-conduction hearing devices. *Hear. Res.* **433**, 108765 (2023).
44. Håkansson, B., Carlsson, P. & Tjellström, A. The mechanical point impedance of the human head, with and without skin penetration. *J. Acoust. Soc. Am.* **80**, 1065–1075 (1986).
45. Dobrev, I. & Sim, J. H. Magnitude and phase of three-dimensional (3D) velocity vector: application to measurement of cochlear promontory motion during bone conduction sound transmission. *Hear. Res.* **364**, 96–103 (2018).
46. Röösl, C., Dobrev, I. & Pfiffner, F. Transcranial attenuation in bone conduction stimulation. *Hear. Res.* **419**, (2022).
47. Eeg-Olofsson, M., Stenfelt, S. & Granström, G. Implications for contralateral bone-conducted transmission as measured by cochlear vibrations. *Otol Neurotol.* **32**, 192–198 (2011).
48. Liyanage, N. et al. Round window reinforcement-induced changes in intracochlear sound pressure. *Appl. Sci.* **11**, (2021).
49. Geerardyn, A. et al. The impact of round window reinforcement on middle and inner ear mechanics with air and bone conduction stimulation. *Hear. Res.* **450**, 109049 (2024).
50. Wils, I., Geerardyn, A., Putzeys, T., Denis, K. & Verhaert, N. Lumped element models of sound conduction in the human ear: a systematic review. *J. Acoust. Soc. Am.* **154**, 1696–1709 (2023).
51. Goode, R. L., Killion, M., Nakamura, K. & Nishihara, S. New Knowledge about the function of the human middle ear: development of an improved analog model. *Am. J. Otol.* **15**, 145–154 (1994).
52. Voss, S. E., Rosowski, J. J., Merchant, S. N. & Peake, W. T. Middle-ear function with tympanic-membrane perforations. II. A simple model. *J. Acoust. Soc. Am.* **110**, 1445–1452 (2001).
53. Zwislocki, J. Analysis of the middle-ear function. Part I: Input Impedance. *J. Acoust. Soc. Am.* **34**, 1514–1523 (1962).
54. Elliott, S. J., Ni, G. & Verschuur, C. A. Modelling the effect of round window stiffness on residual hearing after cochlear implantation. *Hear. Res.* **341**, 155–167 (2016).
55. Rosowski, J. J., Songer, J. E., Nakajima, H. H., Brinsko, K. M. & Merchant, S. N. Clinical, experimental, and theoretical investigations of the Effect of Superior Semicircular Canal Dehiscence on hearing mechanisms. *Otol Neurotol.* **25**, 323–332 (2004).
56. Xue, L. et al. The role of third windows on human sound transmission of forward and reverse stimulations: a lumped-parameter approach. *J. Acoust. Soc. Am.* **147**, 1478–1490 (2020).
57. Stenfelt, S. & Reinfeldt, S. A model of the occlusion effect with bone-conducted stimulation. *Int. J. Audiol.* **46**, 595–608 (2007).
58. Grossöhmichen, M., Salcher, R., Püschel, K., Lenarz, T. & Maier, H. Differential Intracochlear Sound Pressure Measurements in Human Temporal Bones with an Off-the-Shelf Sensor. *Biomed Res. Int.* 1–10 (2016).
59. Nakajima, H. H. et al. Differential Intracochlear Sound pressure measurements in normal human temporal bones. *J. Assoc. Res. Otolaryngol.* **10**, 23–36 (2009).
60. Pfiffner, F. et al. A MEMS condenser microphone-based Intracochlear Acoustic Receiver. *IEEE Trans. Biomed. Eng.* **64**, 2431–2438 (2017).
61. Koch, M. et al. Methods and reference data for middle ear transfer functions. *Sci. Rep.* **12**, 1–17 (2022).
62. Kringlebotn, M. The equality of volume displacements in the inner ear windows. *J. Acoust. Soc. Am.* **98**, 192–196 (1995).
63. Stenfelt, S., Hato, N. & Goode, R. L. Fluid volume displacement at the oval and round windows with air and bone conduction stimulation. *J. Acoust. Soc. Am.* **115**, 797–812 (2004).
64. Putzeys, T. & Wübbenhorst, M. Asymmetric polarization and hysteresis behaviour in ferroelectric P(VDF-TrFE) (76/24) copolymer thin films spatially resolved via LMM. *Phys. Chem. Chem. Phys.* **17**, 7767–7774 (2015).
65. Raufer, S., Gamm, U. A., Grossöhmichen, M., Lenarz, T. & Maier, H. Middle ear actuator performance determined from intracochlear pressure measurements in a single cochlear Scala. *Otol Neurotol.* **42**, e86–e93 (2021).
66. Greene, N. T., Jenkins, H. A., Tollin, D. J. & Easter, J. R. Stapes displacement and intracochlear pressure in response to very high level, low frequency sounds. *Hear. Res.* **348**, 16–30 (2017).
67. Grossöhmichen, M. et al. Validation of methods for prediction of clinical output levels of active middle ear implants from measurements in human cadaveric ears. *Sci. Rep.* **7**, 15877 (2017).
68. Ver Hoef, J. M. Who invented the delta method? *Am. Stat.* **66**, 124–127 (2012).

# Acknowledgements

The authors are grateful to the donors and Dean Prof. Dr. Paul Herijgers and his team of the Vesalius Institute, KU Leuven, for their help in harvesting and preserving the cadaveric heads. This work was supported by Flanders Innovation and Entrepreneurship (HBC.2020.2201), Cochlear Ltd., Research Foundation—Flanders (FWO1SD3322N, FWO1804816N, FWO088619N), KU Leuven (internal funds and IDN/21/021) and Legaat Ghislaine Heylen (Tyberghein).

# Author contributions

All authors designed the experiments. I.W. and A.G. conducted the experiments. A.G. prepared the specimens. I.W. analysed the data. I.W. prepared the figures and drew the schematic in Fig. 1. I.W. wrote the paper. All authors reviewed and approved the manuscript. Funding was obtained by the senior authors.

# Declarations

# Competing interests

GF is employed by Cochlear Ltd. The remaining authors declare no competing interests.

# Additional information

**Supplementary Information** The online version contains supplementary material available at <https://doi.org/10.1038/s41598-024-81505-9>.

**Correspondence** and requests for materials should be addressed to I.W.

**Reprints and permissions information** is available at [www.nature.com/reprints](http://www.nature.com/reprints).

**Publisher's note** Springer Nature remains neutral with regard to jurisdictional claims in published maps and institutional affiliations.

**Open Access** This article is licensed under a Creative Commons Attribution-NonCommercial-NoDerivatives 4.0 International License, which permits any non-commercial use, sharing, distribution and reproduction in any medium or format, as long as you give appropriate credit to the original author(s) and the source, provide a link to the Creative Commons licence, and indicate if you modified the licensed material. You do not have permission under this licence to share adapted material derived from this article or parts of it. The images or other third party material in this article are included in the article's Creative Commons licence, unless indicated otherwise in a credit line to the material. If material is not included in the article's Creative Commons licence and your intended use is not permitted by statutory regulation or exceeds the permitted use, you will need to obtain permission directly from the copyright holder. To view a copy of this licence, visit <http://creativecommons.org/licenses/by-nc-nd/4.0/>.

© The Author(s) 2024